＜ 0riginal Paper ＞ J. Flow Injection Anal., Vol. 34, No. 1 (2017) 11−14

High Throughput Titration Based on Variable and Fixed Triangular Wave Controlled Flow Ratiometry with LED-Photodiode Detector

Naoya Kakiuchi[1], Aiko Miyazaki[2], Akihiro Fujikawa[3], Masaki Takeuchi[1,2,4] and Hideji Tanaka[1,2,4,*]

[1] Graduate School of Pharmaceutical Sciences, Tokushima University, Shomachi 1-78-1, Tokushima 770-8505, Japan

[2] Faculty of Pharmaceutical Sciences, Tokushima University, Shomachi 1-78-1, Tokushima 770-8505, Japan

[3] Shikoku Riken Co., Suzue-Minami 68-1, Kawauchi-cho, Tokushima 771-0124, Japan

[4] Institute of Biomedical Sciences, Tokushima University, Shomachi 1-78-1, Tokushima 770-8505, Japan

Abstract

Unprecedented high throughput flow titration (maximally 43.1 titrations/min) has been realized by a triangular wave controlled flow ratiometry using an in-house LED-photodiode detector. The detector was fabricated mainly with quartz tubing, an LED, a photodiode and a DC power supply. While the total flow rate is held constant, a titrand (acid) is merged with a titrant (base) containing an indicator, the flow rate of which is linearly varied by the control voltage V_c supplied from a computer. Downstream, the intensity of the transmitted light is monitored with the detector and acquired in the computer as detector output voltage V_d. In the initial feedback-based mode, the lamp direction of V_c is changed from upward to downward, or *vice versa*, when the detector senses the equivalence point. In the subsequent fixed triangular wave controlled mode, the scan range and the scan rate of V_c are further limited and quickened, respectively, in order to increase the throughput rate. Equivalence point is determined by offsetting the effect of the lag time between the upstream merging and the downstream sensing. Although the present approach is an absolute method, calibration curves have been constructed for practical operation. The linearity of the curve is satisfactory ($r^2 > 0.993$). The present method is well applicable to various titrations of acids and bases including acetic acid in commercial vinegars.

Keywords Flow titration, flow ratiometry, triangular wave control, high throughput, vinegar

1. Introduction

Titrimetry is one of the classical analytical methods that are still in use widely. In Japanese Pharmacopoeia [1], for example, titrimetry is adopted as the quantification methods for about one half drugs listed in the monograph. Conventional manual titration using glassware is, however, time-consuming and needs considerable amounts of reagents and samples. In addition, the analyst has to pay close attention, especially when the sample and/or reagent are hazardous. Various automated flow titration methods have, therefore, been developed to overcome such drawback of batch titration, as reviewed by Tanaka and Nakano [2]. These include flow injection (FI) titration [3,4], sequential injection (SI) titration [5], flow ratiometry [6,7], triangle programmed coulometric titration [8-10], monosegment flow titration [11] and so on. Lima *et al*. [12] reported a flow-batch hybrid method. They further introduced a digital movie-based detector to their flow-batch analyzer, where hue value was computed from RGB values [13]. These methods mentioned above could reduce the consumption of sample and reagent. They took, however, several tens of seconds or more per titration.

Feedback-based flow ratiometry, first reported by Tanaka *et al*. [14,15], is a sophisticated flow ratiometry, where the error due to the lag time between the upstream titrand-titrant mixing and the downstream sensing of corresponding signal is corrected by a feedback control. Fais *et al*. [16] applied this concept to a process analysis. More recently, Tanaka *et al*. [17-19] further advanced the approach by coupling feedback control and fixed triangular wave control. Unprecedented high throughput rate (maximally 34 titrations/min) was realized with reasonable precision (RSD < 0.5%) [18].

In the present study, this approach has been reexamined to get higher throughput rate using an in-house LED-photodiode detector. The developed system is evaluated by applying it to the determination of acetic acid in commercial vinegars.

2. Experimental

2.1. Regents

Bromocresol Green, 2 mol dm^{-3} hydrochloric acid, 2 mol dm^{-3} sodium hydroxide solution, 25 % ammonia solution and sodium carbonate were purchased from Kanto Chemicals, Tokyo, Japan. Bromothymol Blue, Thymol Blue and Thymolphthalein were purchased from Wako Pure Chemical Industries, Osaka, Japan. The above-mentioned reagents were of analytical reagent grade and were used without further purification. Sartorius Arium 611DI grade deionized water was used throughout. Vinegar samples were purchased at local markets in Tokushima, Japan and 10 times diluted with water prior to the analysis.

2.2. Flow system

Figure 1 shows the flow system of the present study. The system was constructed with two peristaltic pumps $P_{1\text{-}2}$ (Minipuls 3, MP-2, GILSON, U.S.A.), a laptop computer PC (Dynabook Satellite 1850 SA120C/4, Toshiba, Japan) with an A/D-D/A converter (PC-CARD-DAS16/12-AO, Measurement Computing,

* Corresponding author.
E-mail: h.tanaka@tokushima-ac.jp

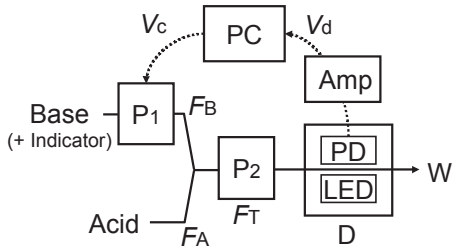

Fig. 1 Flow system
P_1 and P_2, peristaltic pump; D, photometer; PD, photodiode; LED, light emitted diode; Amp, current amplifier; PC, laptop computer with A/D-D/A converter; V_c, controller output voltage; V_d, detector output voltage. F_A, F_B and F_T are acid, base and total flow rates, respectively; W, waste.

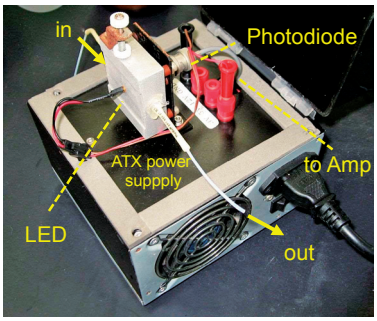

Fig. 2 LED-PD based photometer
Size: 14 cm (W) x 15 cm (D) x 20 cm (H).

U.S.A.), a photometer D (described below) and an amplifier Amp (C2719, Hamamatsu Photonics, Japan). PTFE tubing (1.59 mm o.d., 0.5 mm i.d.) was used as the conduit of the flow system except for pump tubing (3.68 mm o.d., 0.51 mm i.d. Pharmed® tubing). No mixing reactor was used because the rollers of P_2 pump actively facilitated the mixing.

Figure 2 shows the photograph of the in-house photometer, assembled mainly with an ATX power supply (3, 5, 12 V) reused from a discarded computer, a light emitting diode (yellow LED; rated current 25 mA; manufacturer is not clear) purchased from a local electronic parts shop, photodiode (PD; Hamamatsu Photonics S2281, Japan), an optical flow cell (3 mm o.d., 1 mm i.d. quartz tubing), a resistor (330 Ω), an aluminum block that was processed to hold the LED, PD and quartz tubing, and a plastic cover purchased from DAISO, Japan. The light from the LED is made incident in the tubing from the right angle. The optical path length is, therefore, maximally 1 mm. The intensity of the transmitted light is measured with PD.

2.3. Method

The flow rate (F_B) of base solution containing an indicator, fed with P_1, was varied in proportional to the controller output voltage (V_c) supplied from PC *via* the A/D-D/A converter. The total flow rate (F_T) was held constant at 1.41 cm^3 min^{-1} with P_2. Acid solution was, therefore, passively aspirated into the flow system at the flow rate of F_T - F_B and merged with the base solution at the confluence point. The solution was introduced to the flow cell of the detector, where the intensity of the transmitted light was measured. The signal from the detector was amplified by the amplifier and acquired in PC as the detector output voltage V_d as Microsoft Excel format. An

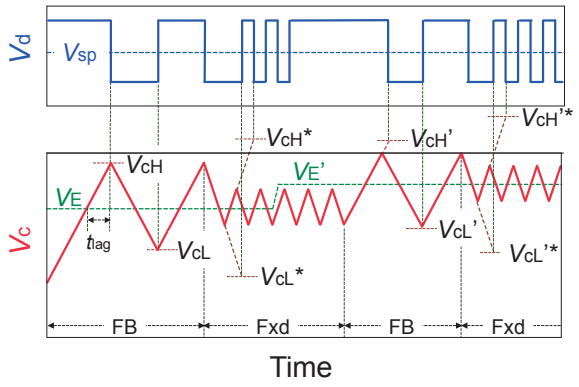

Fig. 3 Principle of high throughput titration by feedback-based variable and fixed triangular wave controlled flow ratiometry
FB, feedback-based mode; Fxd, fixed triangular wave controlled mode; V_c, controller output voltage; V_d, detector output voltage; V_E, controller output voltage that gives equivalence composition at the confluence point; V_{cH} and V_{cL}, maximum and minimum V_c in FB mode, respectively; V_{cH}* and V_{cL}*, maximum and minimum V_c in Fxd mode, respectively; V_{sp}, set point corresponding to V_d at the equivalence point. The symbols with prime (') mean the respective values after the change in sample concentration.

in-house program written in Excel VBA was used to control the system, acquire data, analyze them and display the result automatically.

3. Principle

In the present configuration (Fig. 1), there should be the control voltage V_E that gives the equivalence point at the confluence point. Similar to conventional batch titration, the following relationship based on flow rate should be satisfied at the equivalence point.

$$n_A C_A (F_T - F_B) = n_B C_B F_B, \qquad (1)$$

where n_A and n_B are valences of acid and base, respectively, and C_A and C_B mean the respective concentrations. On the assumption that F_B is proportional to V_c (thus, $F_B = kV_c$, where k is a constant of proportionality), Eq. 1 is rearranged to Eq. 2.

$$\frac{1}{V_E} = \frac{n_B k C_B}{n_A F_T C_A} + \frac{k}{F_T} \qquad (2)$$

The reciprocal of V_E is proportional to C_B or the reciprocal of C_A. Therefore, if V_E is obtained, either of the concentrations can be determined by using the other as the standard.

However, there is a lag time t_{lag} between the upstream mixing and the downstream sensing of corresponding signal. In order to correct the effect of t_{lag}, the principle shown in Fig. 3 is applied. The major principle was described before in detail [17,18]. Briefly, V_c, thus F_B, is linearly increased. Even if V_c reaches V_E, the equivalence signal V_{sp} is not detected because of t_{lag}. After t_{lag}, V_d reaches to V_{sp}. At this instant, the scan direction of V_c is changed downward. Likewise, when V_{sp} is sensed again, the direction is changed upward. By averaging the most recent V_c maximum, V_{cH}, and the minimum, V_{cL}, the effect of t_{lag} is offset and V_E can be obtained. Next, fixed triangular wave control (Fxd) is applied. The amplitude of the

triangular wave is narrower and the scan rate of V_c is faster than those of the feedback (FB) mode in order to increase the throughput rate. Although the scan direction is reversed before the sensing the equivalence point, V_{sp} can be sensed as long as the V_c scan range covers V_E. The values corresponding to V_{cH} and V_{cL} (V_{cH}* and V_{cL}*, respectively) can be estimated by extrapolating V_c to the time when V_{sp} is sensed. When V_E moves outside of the scan range due to the change in sample concentration, feedback control is applied again after some period in order to locate a new equivalence point (V_E'). The period is arbitrarily preset by the operator as a software parameter.

The scan limits of V_c are 5 V and 0 V, respectively. In our previous algorithm [17-19], V_E should be in the range from $t_{lag}\cdot(dV_c/dt)$ to 5 V - $t_{lag}\cdot(dV_c/dt)$, where (dV_c/dt) is the scan rate of V_c, or V_c reaches the limit before the sensing of V_E. In the present study, the program is improved to cover entire V_E (*i.e.*, 0 ~ 5 V) by an extrapolation approach (see V_{cH}' in Fig. 3) similar to that in the Fxd mode, as mentioned above.

4. Results and Discussion

4.1. Optimization of analytical parameters

The scan rate of V_c, dV_c/dt, in FB mode was studied in the range from 0.1 to 0.4 V s^{-1} using 0.1 mol dm^{-3} HCl and the same concentration of NaOH as titrand and titrant, respectively. Higher dV_c/dt is preferable for rapidly locating V_E first time when FB mode is started. The RSD of V_E were *ca*. 0.55 % of in the range of 0.1 – 0.2 V s^{-1}, and became larger at higher dV_c/dt. Therefore, 0.2 V s^{-1} is selected as dV_c/dt in FB mode.

In Fxd mode, the throughput rate is proportional to dV_c/dt. However, repeatability became worse at higher dV_c/dt. That is, RSD of V_E at dV_c/dt of 0.3, 0.4 and 0.5 V s^{-1} (scan range of V_c was 50 % of the latest FB scan range) were 0.57, 0.95 and 2.42 %, respectively. By taking the throughput rate and the repeatability into consideration, 0.4 V s^{-1} was selected as a compromise. Scan range of V_c in Fxd mode also affects the throughput rate. That is, the rate is inversely proportional to the scan range. The scan range of Fxd mode was investigated at 50 %, 40 %, 30 % or 20 % of the latest scan range in FB mode. The time needed per titration was 2.34 s, 2.09 s and 1.39 s, corresponding to the throughput rate of 25.6, 28.6 and 43.1 titrations/min at 50 %, 40 % and 30 %, respectively. The respective RSD of V_E were 0.81 %, 1.28 %, and 7.89 %. The scan range of 20 % of the latest FB mode was too narrow to obtain precise V_E. The throughput rate of 43.1 titrations/min exceeds our previous record (34.1 titrations/min) [18]. However, 40 % was mainly used as the scan range in Fxd mode by taking the repeatability into account.

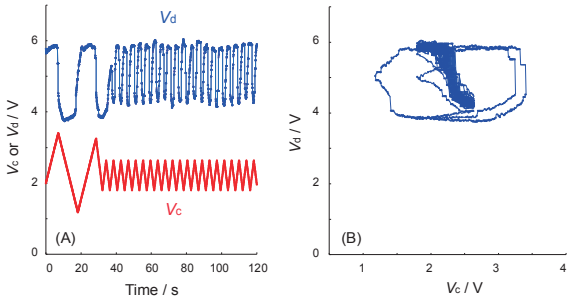

Fig. 4 Temporal profile of V_c and V_d (A) and titration curve (B) for rice vinegar
The analytical concentration of acid as CH_3COOH in the rice vinegar is 796.7 ± 4.3 mmol dm^{-3}. Titrant: 0.1 mol dm^{-3} NaOH. The scan range in Fxd mode is 40 % of that in the latest FB mode.

4.2. Analytical performance

Typical flow signals are shown in Fig. 4(A), where a rice vinegar as an example of real samples is titrated with 0.1 mol dm^{-3} NaOH containing 0.2 mmol dm^{-3} BTB. V_d is recorded and shown in these figures after being amplified by 5 times on the software in addition to the amplification by the current amplifier. Operator can arbitrarily set the amplification factor through the "Parameters" sheet of the Excel software-based file. Sampling frequency is 20 Hz and V_{sp} is 5 V. Obtained V_E is 2.31 ± 0.12 (n = 44) V. The time needed per titration was 2.09 s, corresponding to the throughput rate is 28.6 titrations/min in Fxd mode. Figure 4B shows the titration curve. The outer loop in the V_c range of 1.18 - 3.52 V and the inner loop in 1.80 – 2.64 V correspond to the data obtained in FB mode and Fxd mode, respectively. It shows that the scan range of V_c, especially that in Fxd mode, is limited just the range of interest.

4.3. Calibration curves of various acid-base titrations

The proposed method is an absolute method in principle, so long as the flow rates of F_T and F_B (see Fig. 1) are accurately calibrated. However, the calibration of flow rates is troublesome. Relative method using the calibration curve based on Eq. 2, where V_E^{-1} is plotted as a function of C_A^{-1} or C_B when the titrand is acid or base, respectively, is more practical approach. Various concentrations of acids (HCl, CH_3COOH and H_3PO_4) and bases (NaOH, NH_3 and Na_2CO_3) were titrated with NaOH and HCl, respectively. Acid-base indicators were selected by taking the respective electrolytic dissociation constants, estimated pH at the equivalence point and the color in

Table 1 Calibration curves of various acids and bases

Titrand	Titrant	Indicator	Conc. of titrant / mol dm^{-3}	Linear range / mol dm^{-3}	r^2
HCl	NaOH	BTB	0.01	0.008 – 0.070	0.9945
			0.05	0.030 – 0.400	0.9957
			0.1	0.075 – 0.800	0.9972
CH_3COOH	NaOH	TB	0.1	0.050 – 1.000	0.9980
H_3PO_4 (1st)	NaOH	BCG	0.1	0.075 – 1.000	0.9981
H_3PO_4 (2nd)	NaOH	TP	0.1	0.050 – 0.800	0.9987
NaOH	HCl	BTB	0.1	0.075 – 0.600	0.9935
NH_3	HCl	BCG	0.1	0.025 – 0.400	0.9999
Na_2CO_3 (1st)	HCl	TB	0.1	0.050 – 0.150	0.9935
Na_2CO_3 (2nd)	HCl	BCG	0.1	0.010 – 0.200	0.9997

Indicator: BTB, Bromothymol Blue; TB, Thymol Blue; BCG, Bromocresol Green; TP, Thymolphthalaine.

Table 2 Analysis of commercial vinegar samples

Sample	C_{AcOH} / mmol dm^{-3}	
	Present flow titration	Conventional manual titration
Grain vinegar	714.8 ± 12.3	716.3 ± 4.6
Rice vinegar	796.7 ± 4.3	778.7 ± 1.2
Apple vinegar	772.8 ± 10.2	765.0 ± 5.1

(n = 3)

the base form into consideration. Table 1 shows the summary of the results. As expected, linear range depends on the titrant concentration (see the data for HCl titration with NaOH). That is, lower titrant concentration is more preferable to cover lower titrand concentration range. As shown in the rightmost column, the linearity of the calibration curve is acceptable ($r^2 > 0.993$).

4.4. Application to analysis of vinegar

The present method was applied to the analyses of commercial vinegar samples, because vinegar is familiar cooking ingredient or seasoning. Vinegars have also been used as model samples for evaluating developed system of flow analysis. For example, a discontinuous flow analysis with photometric detection by Cardwell *et al*. [20], a monosegmented flow analysis by Honorato *et al*. [21], a multicommutation – attenuated total reflectance IR spectroscopy by Moros *et al*. [22] and an FI titration with standard addition approach by Wójtorowicz *et al*. [23] were validated through the application to vinegars. González-Rodorígues *et al*. [24] developed an FIA system that incorporated pervaporation device to sequentially determine ethanol and acetic acid in vinegar. Table 2 lists the acidity of vinegars expressed as CH_3COOH concentration, C_{AcOH}, obtained by the present method. As a reference, C_{AcOH} obtained by the conventional manual titration [1] are also shown. Although the reproducibility in the present method is slightly lower than that in the manual titration, the analytical values agree well between them within 3 % in relative error. The distinct advantages of the proposed method over the manual titration are to save time, sample and reagent needed per titration. On the assumption that the manual titration takes 5 min and consumes 10 cm^3 of sample and 20 cm^3 of titrant per titration, the present method saves them to about 1/200, 1/500 and 1/1300, respectively. In Japan, the acidity of vinegar is strictly specified in Japanese Agricultural Standard （JAS） [25]. The present method would be useful in the manufacturing process to quickly detect the product that does not conform the speciation.

In conclusion, the throughput rate of feedback-based variable and fixed triangular wave controlled flow ratiometry has further been advanced with an in-house LED-photodiode detector. The developed system can successfully applied to the analyses of commercial vinegars. Although the scannable range of flow ratio is extended to $0 \sim \infty$ through the improvement in software, linear ranges of the calibration curves are almost comparable to the previous results [18], presumable because the error becomes larger as the titrand/titrant flow ratio approaches to 0 or ∞. The axial dispersion also affect the results, especially when the concentration difference between titrand and titrant is large. The introduction of air segmentation approach to the present flow ratiometry is expected to limit the axial dispersion and thus to widen applicable range. Such concept is currently under investigation.

5. Acknowledgements

The present study is partly supported by the Grant-in-Aid for Scientific Research (C) (15K07889) from the Japan Society for the Promotion of Sciences (JSPS).

References

[1] The Japanese Pharmacopoeia, 17th ed., Part. 1, "*Official Monograph*", **2016**, The Ministery of Health, Labor and Welfare, Tokyo.
[2] H. Tanaka and S. Nakano, *J. Flow Inject. Anal*., **2004**, *21*, 123.
[3] A. U. Ramsing, J. Ruzicka, and E. H. Hansen, *Anal. Chim. Acta*, **1981**, *129*, 1.
[4] J. Ruzicka, and E. H. Hnasen, "*Flow injection analysis*", 2nd ed., **1988**, John Wiley & Sons, New York, pp. 229-242.
[5] J.F. van Staden, and H. du Plessis, *Anal. Commun.*, **1977**, *34*, 147.
[6] W. J. Blaedel and R. H. Laessig, *Anal. Chem.*, **1964**, *36*, 1617.
[7] W. J. Blaedel and R. H. Laessig, *Anal. Chem.*, **1965**, *37*, 332.
[8] G. Nagy, K. Tóth, and E. Pungor, *Anal. Chem*., **1975**, *47*, 1460.
[9] G. Nagy, Z.S. Fehér, K. Tóth, and E. Pungor, *Anal. Chim. Acta*., **1977**, *91*, 87 and 97.
[10] U. Spohn, G. Nagy, and E. Pongor, *Anal. Sci*., **1986**, *2*, 423 and 431.
[11] J. Marcos, A. Ríos, and M. Valcárcel, *Anal. Chim. Acta*., **1992**, *261*, 489 and 495.
[12] R. S. Honorato, M. C. U. Araújo, R. A. C. Lima, E. A. G. Zagatto, R. A. S. Lapa, and J. L. F. C. Lima, *Anal. Chim. Acta*, **1999**, *396*, 91.
[13] R. A. C. Lima, L. F. Almeida, W. S. Lyra, L. A. Siqueira, E. N. Gaiao, S. S. L. Paiva Junior, and R. L. F. C. Lima, *Talanta*, **2016**, *147*, 226.
[14] H. Tanaka, P. K. Dasgupta, and J. Huang, *Anal. Chem*., **2000**, *72*, 4713.
[15] P. K. Dasgupta, H. Tanaka, and K. D. Jo, *Anal. Chim. Acta*, **2001**, *435*, 289.
[16] M. Fais, C. Schwarz, and F. C. Leinweber, *Chem. Ing. Tech*., **2016**, *88*, 793.
[17] H. Tanaka and T. Baba, *Talanta*, **2005**, *67*, 848.
[18] H. Tanaka and T. Baba, *Anal. Sci.*, **2005**, *21*, 615.
[19] T. Aydan, A. Kitagawa, M. Takeuchi, and H. Tanaka, *J. Flow Inject. Anal*., **2008**, *25*, 65.
[20] T. J. Cardwell, R. W. Cattrall, G. J. Cross, G. R. O'Connell, J. D. Petty, and G. R. Scollary, *Analyst*, **1991**, *116*, 1051.
[21] R. S. Honorato, M. C. U. Araujo, G. Veras, E. A. G. Zagatto, R. A. S. Lapa, and J. L. F. C. Lima, *Anal. Sci*., **1999**, *15*, 665.
[22] J. Moros, F.A. Iñón, S. Garrigues, and M de la Guardia, *Talanta*, **2008**, *74*, 632.
[23] M. Wójtorowicz, J. Kozak, D. Gornacka, and P. Koscielniak, Anal. Sci., **2008,** *24*, 1593.
[24] J. González-Rodorígues, P. Pérez-Juan, and M. D. L. de Castro, Analyst, **2001**, *126*, 117.
[25] JAS, "Japanese Agricultural Standard for Brewed Vinegar", **2016**, Ministry of Agriculture, Forestry and Fisheries, Japan.

(Received July 10, 2017)
(Accepted August 18, 2017)